



DELFT UNIVERSITY OF TECHNOLOGY

SC42145 ROBUST CONTROL

PART 2 Multi variable Mixed-Sensitivity

1 Part 2

The objective of this part of the assignment is to design a Mixed-Sensitivity centralized controller for the floating wind turbine. In the first part of this report, we consider both channels as control inputs: the pitch angle $\beta[\text{rad}]$ and the generator torque $\tau_e[\text{Nm}]$, and both outputs of the system: the generator speed $\omega_r[\text{rad/s}]$ and fore-aft tower top displacement $z[\text{m}]$. The state space system provided is:

$$\dot{x} = \begin{bmatrix} -0.4220 & -0.2204 & 0 & -0.2204 & 0 \\ 0.0233 & -0.0109 & -0.0400 & -0.0096 & 0 \\ 0 & 1.0000 & 0 & 0 & 0 \\ 0.1455 & -0.0598 & 0 & -0.1651 & -10.8232 \\ 0 & 0 & 0 & 1.0000 & 0 \end{bmatrix} x + \begin{bmatrix} -0.0799 & -0.0096 \\ -0.0067 & 0 \\ 0 & 0 \\ -0.0420 & 0 \\ 0 & 0 \end{bmatrix} u$$

$$y = \begin{bmatrix} 1 & 0 & 0 & 0 & 0 \\ 0 & 0 & 1 & 0 & 1 \end{bmatrix} x + 0u$$

where

$$x = \begin{bmatrix} \omega_r \\ \dot{z}_1 \\ z_1 \\ \dot{z}_2 \\ z_2 \end{bmatrix}, u = \begin{bmatrix} \beta \\ \tau_e \end{bmatrix}, y = \begin{bmatrix} \omega_r \\ z \end{bmatrix}$$

Using the MATLAB command **ss2tf** and splitting the system into four subsystems corresponding to different inputs and outputs, we represent this state space system as a matrix of transfer functions. The corresponding transfer functions of the plant are:

$$G(s) = \begin{bmatrix} \frac{-0.079878(s^2 - 0.007693s + 0.04)(s^2 + 0.0492s + 10.82)}{(s+0.4104)(s^2 + 0.02113s + 0.04101)(s^2 + 0.1664s + 10.85)} & \frac{-0.048738(s+0.6986)(s^2 + 0.01562s + 1.527)}{(s+0.4104)(s^2 + 0.02113s + 0.04101)(s^2 + 0.1664s + 10.85)} \\ \frac{-0.0095639(s^2 + 0.01085s + 0.04)(s^2 + 0.1651s + 10.82)}{(s+0.4104)(s^2 + 0.02113s + 0.04101)(s^2 + 0.1664s + 10.85)} & \frac{-0.0016139(s^2 + 0.01562s + 1.527)}{(s+0.4104)(s^2 + 0.02113s + 0.04101)(s^2 + 0.1664s + 10.85)} \end{bmatrix}$$

1.1 QUESTION 1

The Relative Gain Array is a measure of the amount of directionality or the amount of coupling in a plant. It is mathematically defined as:

$$RGA(G) = \Lambda(G) \triangleq G \times (G^{-1})^T \quad (1)$$

here \times represents the Hadamard product.

The RGA can be computed using the MATLAB command $G.*pinv(G)'$ where the gain of G at $w=0$ and $w=0.4*2*\pi$ needs to be computed. Using the MATLAB codes

$$RGA_{w0} = evalfr(G, 0). * pinv(evalfr(G, 0))' \quad (2)$$

$$RGA_{w0.4*2*\pi} = evalfr(G, 0.4 * 2 * \pi * i). * pinv(evalfr(G, 0.4 * 2 * \pi * i))' \quad (3)$$

Note that we give a complex input for the frequency, as the resultant RGA values should be complex. For $w=0$ and $w=0.4*2*\pi$ respectively, we get:

$$RGA_{w0} = \begin{bmatrix} -0.6554 & 1.6554 \\ 1.6554 & -0.6554 \end{bmatrix} \quad (4)$$

$$RGA_{4*2*\pi} = \begin{bmatrix} -0.0117 + 0.1068i & -0.9217 - 0.4306i \\ 0.9729 - 0.2973i & -0.0034 + 0.1074i \end{bmatrix} \quad (5)$$

The values are around 1 and much less than 10. This means that there is moderate coupling(i.e. moderately easy to control/moderately sensitive to uncertainty) between the input β and output z . For instance, if we consider the RGA value between β and z for $w=0.4 * 2 * \pi$, we observe that it is equal to $0.9729 - 0.2973i$, which is close to 1 in magnitude. Since we prefer to have pairings that are non-negative and as close to 1 as possible, it means that for $w=0$ (steady state), we prefer to control w_r using τ_e , and for $w=0.4 * 2 * \pi$, we prefer to control z using β .

1.2 QUESTION 2

In order to obtain the MIMO poles and zeros, we need to compute the poles and zeros of the determinant of the minimal realization transfer function of matrix G in equation. We compute this determinant to ensure that there are no hidden poles and zeros. We use the command

$$\text{pole}(\text{minreal}((G(1,1) * G(2,2)) - (G(1,2) * G(2,1))), 0.0001)) \quad (6)$$

and

$$\text{tzero}(\text{minreal}((G(1,1) * G(2,2)) - (G(1,2) * G(2,1))), 0.0001)) \quad (7)$$

to find the poles and zeros. The 0.0001 is an argument for **minreal** function, which is the tolerance used for state elimination or pole-zero cancellation.

The results are zeros = $[-0.0078 \pm 1.2358i]$ and poles = $[-0.0832 \pm 3.2936i, -0.0106 \pm 0.2022i, -0.4104]$. Since all the poles and zeros have negative real value and are in the LHP (Left Half Plane), G is a stable MIMO system and has no unstable hidden modes that could cause instability of closed loop system.

1.3 QUESTION 3

The standard form of W_{p11} is

$$W_{p11} = \frac{\frac{s}{M_i} + w_{Bi}}{s + w_{Bi}A_i} \quad (8)$$

where M_i is the \mathcal{H}_∞ norm of the sensitivity function with the provided value of 1.8, w_{Bi} is the bandwidth ($2*\pi*\text{cut-off frequency}$), with the value of $0.4*2*\pi$, A_i is the attenuation of low-frequency disturbances with the value of 10^{-4} .

After substituting the corresponding values, the transfer function of W_{P11} is

$$W_{p11} = \frac{\frac{s}{1.8} + 0.8 * \pi}{s + 0.8 * \pi * 10^{-4}} \quad (9)$$

1.4 QUESTION 4

The block diagram of a standard generalized plant is as shown in Figure 1. where w are the exogenous

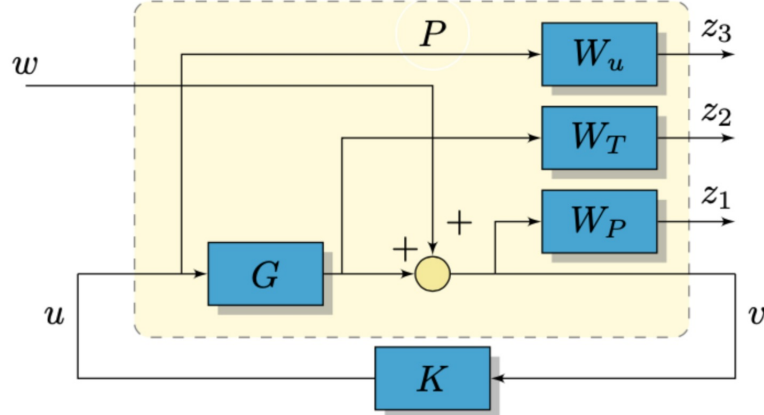


Figure 1: Standard Generalized MIMO Plant

input signals [d; r; n] where d is the disturbance input, r is the reference input and n is the measurement input. v is the error or $r - y_{in}$. u is the controller output or the control signals. G is the plant, and K is the controller. z are the exogenous outputs. W_u , W_t and W_p are the controller weights, output weights and error weights respectively. For our plant, we don't control the output weight, just the controller weights and error weights. Our generalized plant is as shown in Figure 2.

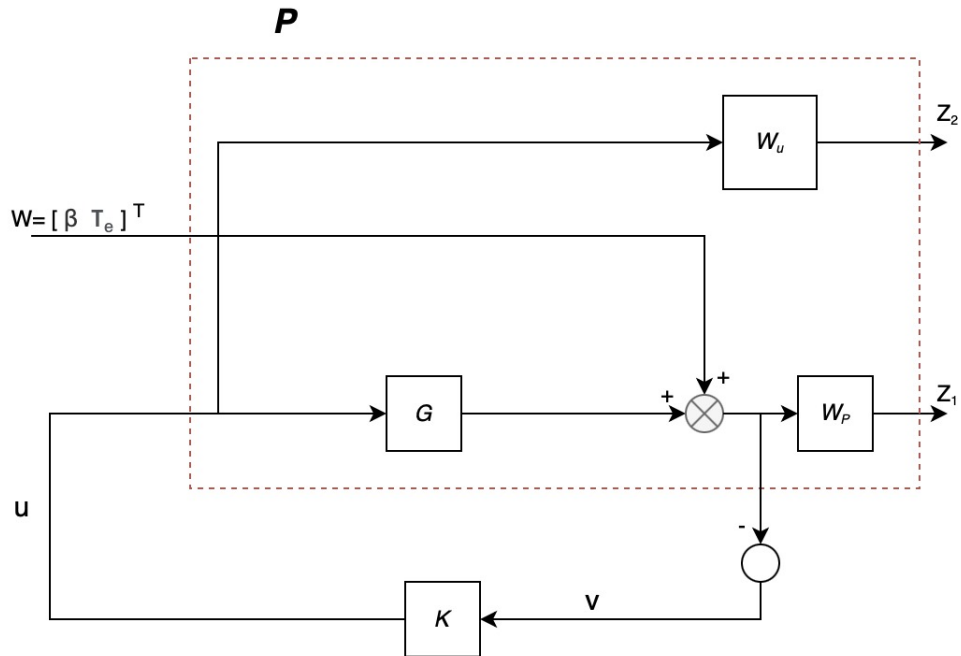


Figure 2: Generalized plant for our Floating Wind Turbine Case

The performance signals are : $z_1 = W_p w - W_p Gu$, and $z_2 = W_u u$, where $w = \begin{bmatrix} \beta \\ \tau_e \end{bmatrix}$, $W_p = \begin{bmatrix} \frac{s}{1.8} + 0.8\pi & 0 \\ \frac{s}{s+0.8\pi*10^{-4}} & 0 \\ 0 & 0.2 \end{bmatrix}$,

$$W_u = \begin{bmatrix} 0.01 & 0 \\ 0 & \frac{5*10^{-3}s^2 + 7*10^{-4}s + 5*10^{-5}}{s^2 + 14*10^{-4}s + 10^{-6}} \end{bmatrix}$$

1.5 QUESTION 5

The symbolic expression of our generalized plant is

$$\begin{bmatrix} z_1 \\ z_2 \\ v \end{bmatrix} = \begin{bmatrix} W_p & -W_p G \\ 0 & W_u \\ I & -G \end{bmatrix} \begin{bmatrix} w \\ u \end{bmatrix} \quad \text{with } w = \begin{bmatrix} \beta \\ \tau_e \end{bmatrix}. \quad (10)$$

The corresponding block diagram is as shown in Figure 2. To elaborate further, this means the generalized plant P takes in 4 inputs(2 exogenous inputs at w, 2 control inputs at u) and produces 6 outputs(4 exogenous outputs- 2 at z_1 , 2 at z_2 , and 2 error signals at v). The mathematical description is covered in the previous question. After applying the **minreal** and **balreal**(to compute balanced realisation) command to the generalized plant, the number of states are 8, which is as expected. The states number of the generalized plant is expected from the fact that G has 5 states, W_p has 1 pole which adds 1 state, and W_u has 2 poles which adds 2 states. Thus in total, the generalized plant should have 8 states.

1.6 QUESTION 6

The performance weights W_p and W_u give an upper bound on the sensitivity and the control sensitivity function respectively. These weights are needed to calculate $\|N\|_\infty$ (robust performance), and ensure that it stays <1 , as desired. These bounds are important because by using them we can control the bandwidth, which means that the larger this bandwidth is, the faster is our step response (i.e. time specification is more easily satisfied).

The diagonal terms of W_u are the penalties imposed on the control inputs. The first diagonal term imposes a penalty on β and the other diagonal term imposes on τ_e .

$$W_u = \begin{bmatrix} 0.01 & 0 \\ 0 & \frac{5*10^{-3}s^2 + 7*10^{-4}s + 5*10^{-5}}{s^2 + 14*10^{-4}s + 10^{-6}} \end{bmatrix}$$

This means that a constant penalty of 0.01 is applied on all frequencies of β from the controller. The bode plot of the controller weight for τ_e is as shown in Figure 3.

The penalty imposed on τ_e is a low pass filter with cut-off frequency approximately 0.0021 rad/s.

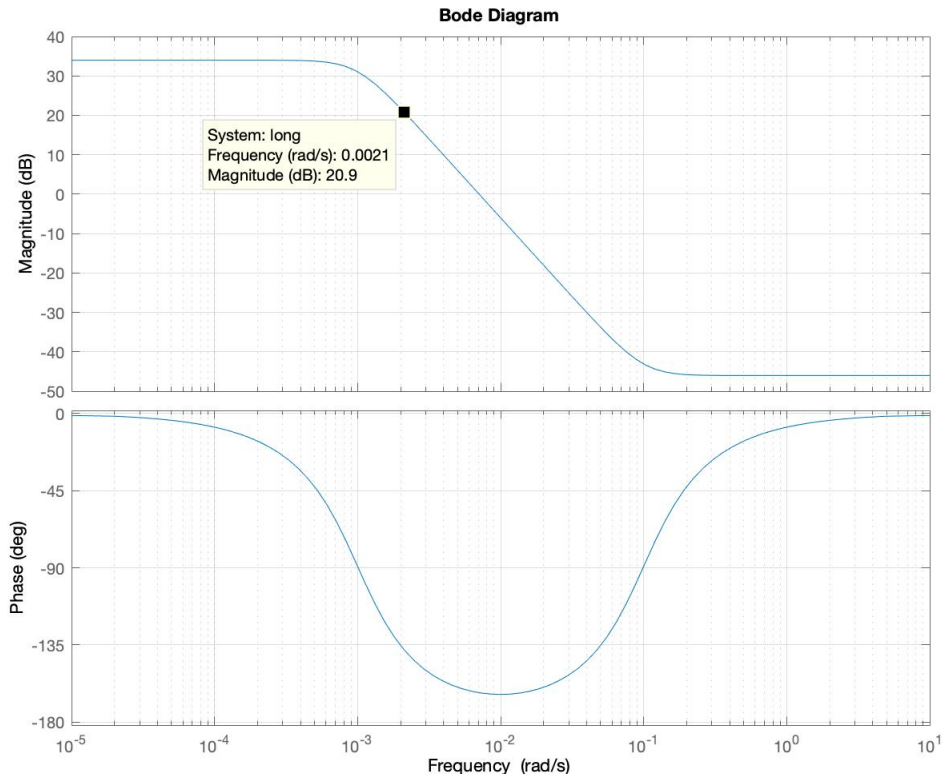


Figure 3: Bode plot of τ_e control input weight

This means that τ_e is desired to operate at high frequencies, where the penalty is less.

The diagonal terms of W_p are the penalties imposed on the errors. The first diagonal term imposes a penalty on w_r and the other diagonal term imposes on z .

$$W_p = \begin{bmatrix} \frac{s}{1.8} + 0.8\pi & 0 \\ \frac{0.8\pi*10^{-4}}{s+0.8\pi*10^{-4}} & 0 \\ 0 & 0.2 \end{bmatrix}$$

This means that a constant penalty of 0.2 is applied on all frequencies of errors of z . The bode plot of the error weight for w_r (W_p11) is as shown in Figure 4.

The penalty imposed on w_r is a low pass filter with cut-off frequency approximately 0.0021 rad/s. This means that errors of w_r are more permissible at higher frequencies, since the penalty is less,

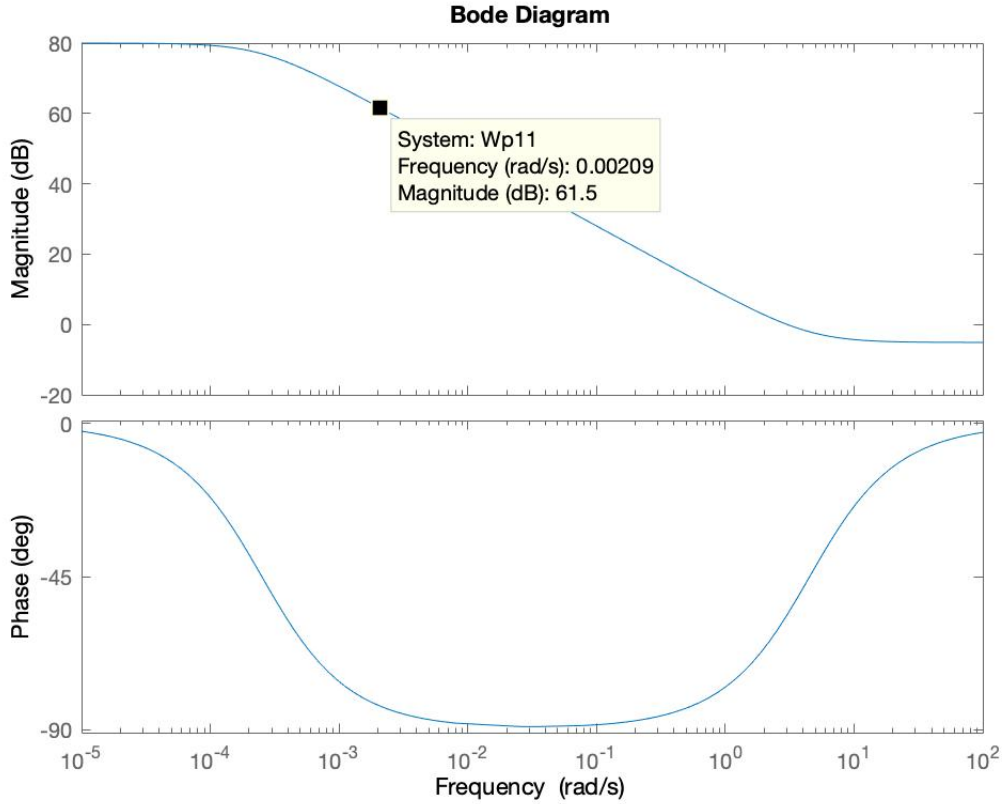


Figure 4: Bode plot of Wp11 error weight

while there is a relatively low penalty for errors in computing z .

Relating this to introductory text in the question, although τ_e is the second controllable input, since we want to keep the static power curve unchanged, we want τ_e to have no role in the steady state. This means that at low frequencies, τ_e should be penalised heavily, and that is exactly what the low pass filter does. Since we want to have a static power curve, it means that $\tau_e \cdot w_r$ should remain static. Therefore, at steady state, the low pass filter at W_p ensures that there are less errors, hence keeping the curve relatively unchanged.

1.7 QUESTION 7

By MATLAB command *hinfsyn*, we obtain the \mathcal{H}_∞ controller K. Applying it to the generalized plant, the open loop is defined as $L = G * K$. Based on the Cauchy's argument principle, for the closed-loop system be internally stable, the generalized Nyquist plot of $\det(I + L)$ should encircle origin N=Z-P times clock wise. Z is the number of the unstable closed loop poles and P is the number of the unstable open loop poles.

In our case, the poles of the closed loop system and open loop system are respectively shown in Table 1. It is clear that Z=0 since the number of the unstable closed loop poles is 0, and P=2 since the number of the unstable open loop poles are 2. Thus the generalized Nyquist plot of $\det(I + L)$ should encircle origin N=0-2 times clock wise, which is 2 times anti-clock wise.

Table 1: Poles of the close loop system and open loop system

Poles of the closed loop system	Poles of the open loop system
-34.8156	-36.6896
-0.0692 + 3.4569i	0.0145 + 3.4460i
-0.0692 - 3.4569i	0.0145 - 3.4460i
-1.6415	-0.0671 + 0.2130i
-0.0933 + 0.2221i	-0.0671 - 0.2130i
-0.0933 - 0.2221i	-0.0572 + 0.0636i
-0.0636 + 0.0601i	-0.0572 - 0.0636i
-0.0636 - 0.0601i	-0.0003

By using the Matlab command *nyquist*, the generalized Nyquist plot of $\det(I + L)$ is shown below:

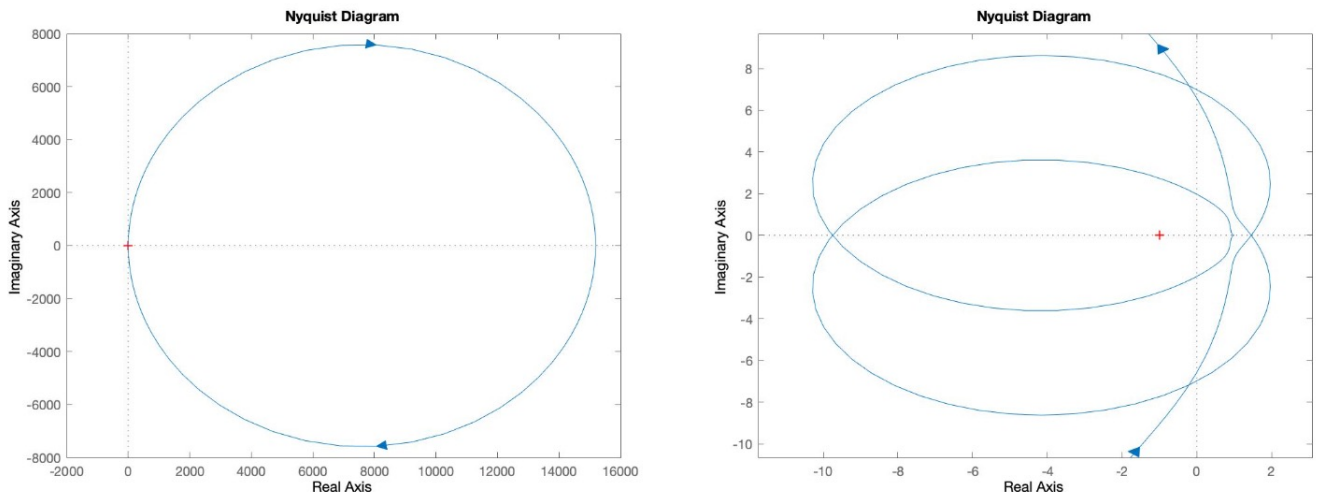


Figure 5: Nyquist plot of $\det(I + L)$ and its zoomed plot

As seen above, the Nyquist plot encircles origin 2 times anti-clock wise, which affirms that the closed-loop system is internally stable.

The \mathcal{H}_∞ controller K has 8 states, which is the same as the number of states of the generalized plant. The number of states regarding the controller is equal to the sum of the number of the states of G(5 states), number of states of W_u (2 states), and number of states of W_p (1 state). The controller K we obtain is shown in Figure 7 and the Bode plot is as shown in Figure 6. The controller K is unstable as it possesses a double conjugate pole at $0.0083 \pm 3.426i$. This renders the open loop system(GK) unstable too, but the closed loop system is stable. The controller K takes in 2 inputs(weighted error

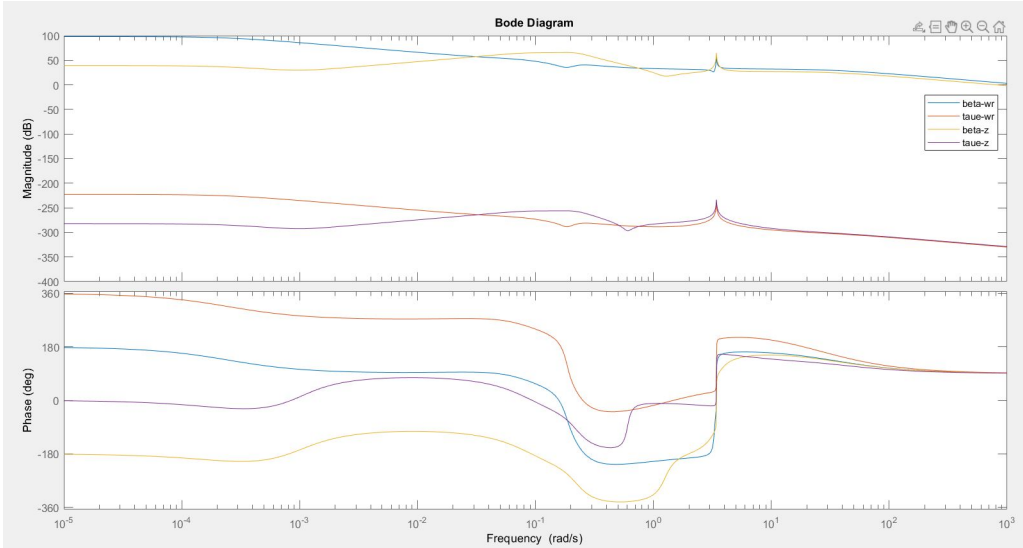


Figure 6: Bode plots of mixed sensitivity controller K

```

From input 1 to output...
-1410 s^7 - 1282 s^6 - 1.563e04 s^5 - 1.143e04 s^4 - 1994 s^3 - 386.9 s^2 - 67.16 s - 2.933
1: -----
s^8 + 34.28 s^7 + 19.71 s^6 + 404.8 s^5 + 100.5 s^4 + 29.11 s^3 + 2.686 s^2 + 0.1467 s + 3.67e-05

-808.4 s^7 - 1651 s^6 - 1.121e04 s^5 - 7973 s^4 - 1.569e04 s^3 - 3345 s^2 - 4.668 s - 0.003323
2: -----
s^8 + 34.28 s^7 + 19.71 s^6 + 404.8 s^5 + 100.5 s^4 + 29.11 s^3 + 2.686 s^2 + 0.1467 s + 3.67e-05

From input 2 to output...
-3.174e-14 s^7 + 3.563e-13 s^6 + 1.266e-12 s^5 + 1.04e-12 s^4 + 1.859e-13 s^3 + 3.767e-14 s^2 + 6e-15 s + 2.623e-16
1: -----
s^8 + 34.28 s^7 + 19.71 s^6 + 404.8 s^5 + 100.5 s^4 + 29.11 s^3 + 2.686 s^2 + 0.1467 s + 3.67e-05

-3.594e-14 s^7 - 3.411e-13 s^6 + 3.584e-12 s^5 + 9.108e-13 s^4 + 1.38e-12 s^3 + 2.755e-13 s^2 + 3.57e-16 s + 2.835e-19
2: -----
s^8 + 34.28 s^7 + 19.71 s^6 + 404.8 s^5 + 100.5 s^4 + 29.11 s^3 + 2.686 s^2 + 0.1467 s + 3.67e-05

```

Figure 7: H_∞ controller K

signals), and gives out 2 outputs(weighted control signals).

1.8 QUESTION 8

The step responses of the close loop of generalized plant with mixed-sensitivity controller are shown in Figure 8 below. Meanwhile, statistical information of the responses are illustrated in Figure 9. The reason why the responses corresponding to the second input τ_e is zero is that the \mathcal{H}_∞ controller we constructed is designed to have second input channel to be nearly zero to meet the control target that the second control input is not allowed to have a static contribution. This is done through the controller and error weights previously defined. Thus, a unit step change in the wind disturbance channel results in $\lim_{t \rightarrow \infty} \tau_e(t) \rightarrow 0$. As we can observe from Figure 9, the response of the close loop

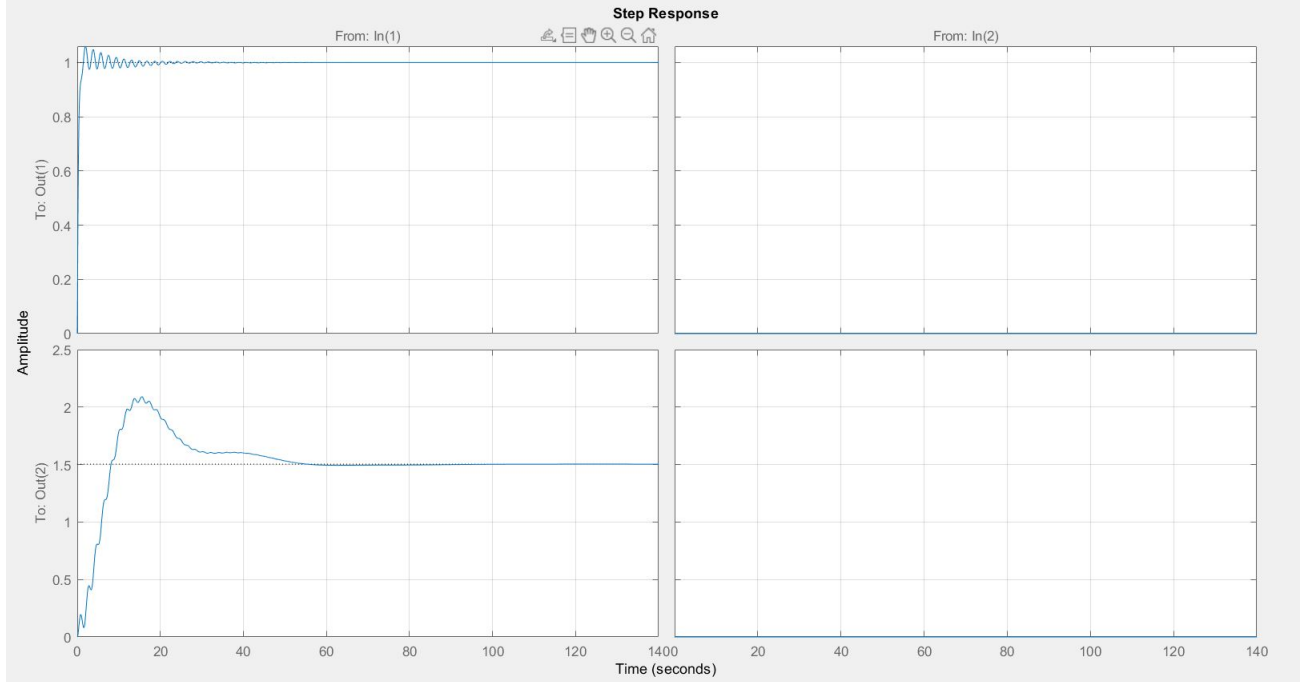


Figure 8: Reference tracking for Closed Loop System with the Mixed-Sensitivity controller

system is relatively fast with small values of settling time. Furthermore, the settling time regarding the first output w_r is much faster than the one of second output z both to the input β .

The stand-out takeaway from Figure 8 is the steady state values of the step responses. w_r settles at 1, as desired for reference tracking. However, z , which is the fore-aft tower displacement settles at 1.5035. The reason for this steady state error is that when the blades pitch at angle β , they there is a temporary minor displacement z which tilts the weight of the turbine backwards. Due to this, there is a torque created due to the weight, which is neutralized by the weighted float. However, the force due to the weight at the tilt, leads to a permanent displacement backwards along the x-axis. This is the reason for the steady state error(since the initial and final position of the tower are different).

As for disturbance rejection, the step responses of the closed loop system is shown in Figure 10, and statistical information of responses are demonstrated in Figure 11.

Similar to reference tracking, the response with respect to the first output ω_r is also much faster than the output z . Even in this case, there is a steady state error for the output z . While it should ideally settle at 0, it settles at -0.23. The reason for it is that when there is a wind disturbance, a force is exerted on the wind turbine which produces a backward displacement of the whole turbine, thus leading to a permanent change in value of z .

The fundamental limitations of the design are:

- The mixed-sensitivity controller itself is unstable due to two poles in RHP, which renders the open loop system unstable as well. However, the close loop system is stable.

```

struct with fields:
    RiseTime: 0.5952
    SettlingTime: 10.3542
    SettlingMin: 0.9001
    SettlingMax: 1.0602
    Overshoot: 6.0283
    Undershoot: 0
    Peak: 1.0602
    PeakTime: 1.9877

ans =
struct with fields:
    RiseTime: 7.0531
    SettlingTime: 49.7757
    SettlingMin: 1.4680
    SettlingMax: 2.0792
    Overshoot: 38.2925
    Undershoot: 0
    Peak: 2.0792
    PeakTime: 15.2502

```

Figure 9: Step Response Information for Reference tracking of Close Loop System

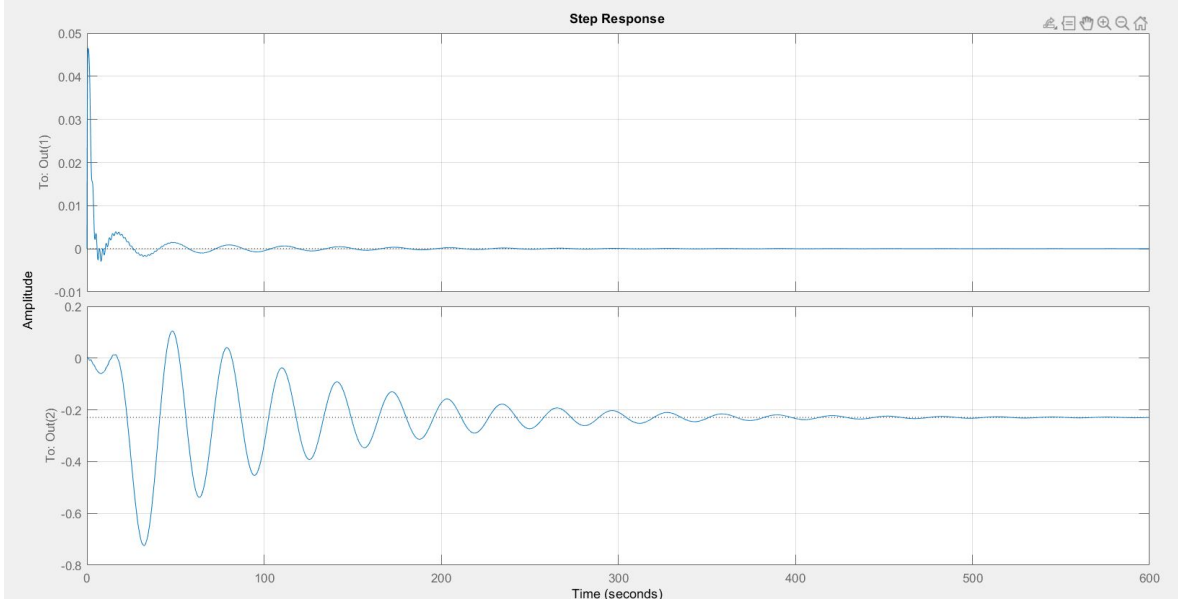


Figure 10: Disturbance rejection of close loop of generalized plant with mixed-sensitivity controller

- With MIMO mixed sensitivity controllers, we cannot intuitively know the side effects of a change on a particular parameter. For instance, if we increase the order of W_p on its denominator to penalize the sensitivity more on low frequencies, we have no intuitive idea on how much would it increase $|W_{pS}|$ (or even decrease), so we have to go through multiple trial and error sessions which is time consuming. In addition, unlike control elements of SISO, weight functions are not standardized and it takes a lot of experience to know what kind of weight should be designed in order to achieve a desired objective.
- The mixed-sensitivity controllers can be of high order (in our case we have a controller of order 8). This means that MIMO controllers are hard to implement in real life, and are also more computationally costly.

```
struct with fields:  
  
    RiseTime: 1.2740e-04  
    SettlingTime: 66.6976  
    SettlingMin: -0.0029  
    SettlingMax: 0.0465  
    Overshoot: 1.3466e+05  
    Undershoot: 8.4072e+03  
    Peak: 0.0465  
    PeakTime: 0.6766  
  
ans =  
  
struct with fields:  
  
    RiseTime: 18.6961  
    SettlingTime: 390.3664  
    SettlingMin: -0.7226  
    SettlingMax: 0.1034  
    Overshoot: 215.0316  
    Undershoot: 45.0804  
    Peak: 0.7226  
    PeakTime: 31.7930
```

Figure 11: Step response information of Disturbance rejection of close loop system

2 Part 2.1- MIMO Weighting Design

The objective of this part of the assignment is to alternatively design Mixed-Sensitivity controllers specifically for non-linear disturbance rejection inputs. Here we assume that the wind turbine runs at its rated power. The power is defined as $w_r \cdot \tau_e$. Thus, to keep the power constant, any changes in w_r need to be counteracted using the control inputs β and τ_{ue} . These changes are brought about by the disturbance, and thus we need to design a system that can successfully reject the disturbance. The disturbance input is essentially in the form of a low frequency sinusoid with a period of around 1000 seconds, and a high frequency turbulence with an average period of around 5 seconds. Since blade pitching is a slow operation, we use τ_e to counteract the changes caused by the high frequency wind speeds, and we use β for low frequency control. β has no effect on the power generation, while the change in generator torque temporarily alters the power. For this case, we only take w_r as the output, and our objective is to design the controller weights W_u and error weights W_p such that the system filters the frequencies as desired, and successfully rejects the disturbance.

2.1 Question 1

The generalised plant for our implementation is as shown in Figure 12. In our implementation, we

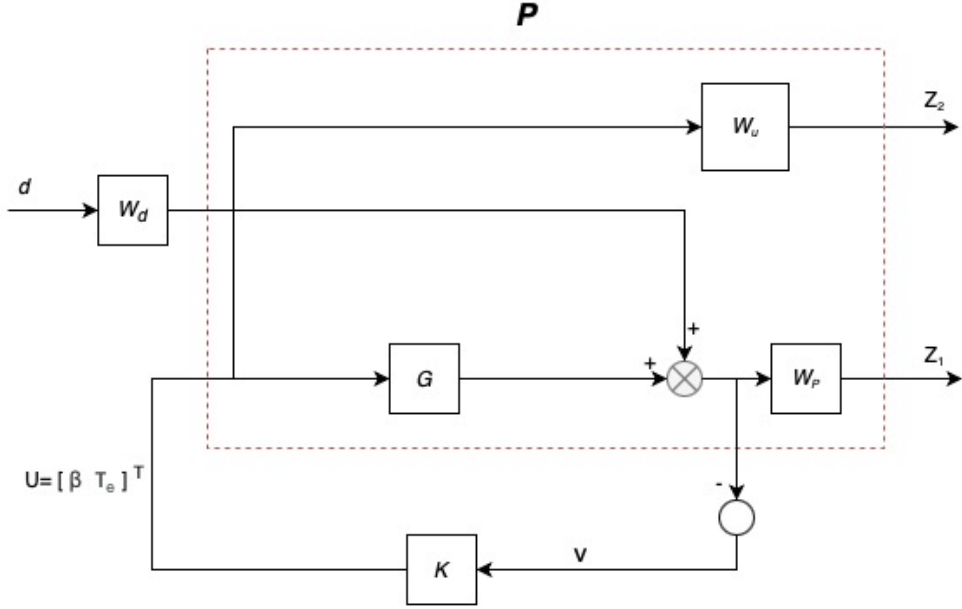


Figure 12: Generalized plant for MIMO weighting Design problem

do not consider G_d as a part of the generalised plant P , since the addition of the disturbance transfer function to this plant, increases the sensitivity a lot. This makes the plant extremely sensitive, and less robust. So to maintain the robustness, G_d is not considered while designing the H_∞ controller. The exogenous input to our plant in this case is the disturbance, which is one input. The control inputs to the plant are β and τ_e . The exogenous outputs of the plant are the weighted control inputs, and the weighted error. Lastly, the error is $-w_r$, which is an input to the controller K . To summarize, our generalised plant P has 3 inputs(d, β, τ_e), and 3 outputs(z_2, z_1 and w_r). The controller takes in one input($-w_r$), and returns 2 outputs(β, τ_e). The plant G takes in 2 inputs from the controller(β, τ_e), and returns r as the output. The disturbance(wind-speed) is added to the output from the plant.

2.2 Question 2

W_p or the error weight will be just a single transfer function in this case, since we have only one output w_r from the plant. A common choice of W_p is

$$W_p = \left[\frac{\frac{s}{M} + w_B}{s + w_B A} \right]$$

where M is the desired bound on the sensitivity function S , w_B is the desired closed loop bandwidth and A is the desired disturbance attenuation inside the bandwidth. These parameters allow us to decide the shape and the peak of the function we use to bound our sensitivity function. W_p is also known as the sensitivity weight since the robust performance N is partially defined as $W_p S$. For optimal, robust performance we require $\|N\|_\infty < 1$, and thus $\|W_p S\|_\infty < 1$. Since we have not included G_d (the Disturbance TF) as a part of the generalized plant, our sensitivity function will be $G_d * \text{inv}(1+GK)$ or $G_d S$. The bode plot of this function is as shown in Figure 13. Our objective is to

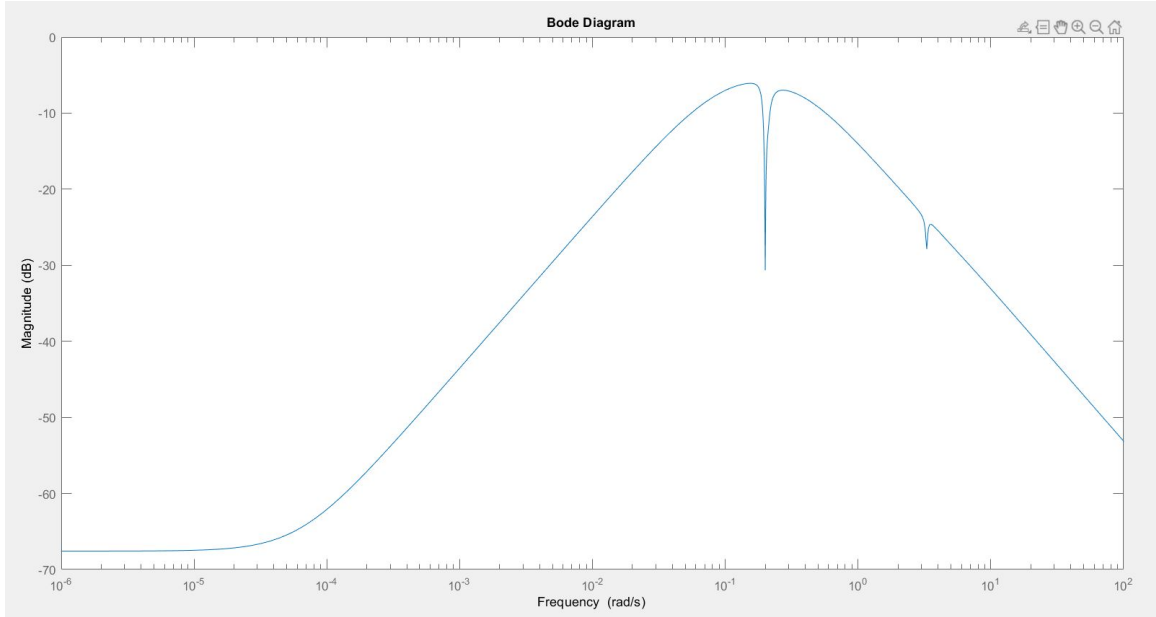


Figure 13: Bode plot of $G_d S$

design an error weight that can keep $G_d S$ bounded. Following the general format of designing W_p as previously mentioned, we choose M as a standard 1.5, A as 10^{-4} , and now we need a desired closed bandwidth w_B in order to bound the sensitivity curve and ensure robust performance. However, choosing w_B has its limitations too. W_p sets a lower bound on the bandwidth. We cannot choose some values w_B since the sensitivity becomes worse as w_B increases, which is undesirable. Thus, the value most found to maintain robustness within limits, is around 0.1Hz or around 0.2π . Any increase in this value leads to the an increase in the sensitivity of the system. The bode plot of the W_p weight along with the system sensitivity is shown in Question 4. Thus, the W_p function we finally chose is:

$$W_p = \left[\frac{\frac{s}{1.5} + 0.2\pi}{s + 0.2\pi \cdot 10^{-4}} \right]$$

This is how we related the gain of our W_p weights to the relation between the input and output transfer function(i.e. $G_d S$). Thus, using the weight mentioned above, we achieve $\|W_p G_d S\|_\infty < 1$ as desired, with some limitations.

Another characteristic of this error weight W_p is that it has the structure of a low pass filter(it imposes a high penalty on low frequency inputs, and a low penalty on high frequency inputs), which makes sense since low frequency disturbance rejection is a slow process which is taken care of by the pitch angle, however a multitude of high frequencies need to be dealt with, which is delegated to the generator torque. Even the selected bandwidth frequency of 0.1Hz, is a high frequency value corresponding to a lower limit on time periods of the high frequency disturbance signals provided in Wind_Data. Thus, this error weight serves as an impetus towards high frequency error control.

2.3 Question 3

The controller K provides 2 outputs to the plant G, one is β , and the other is τ_e . These act as control inputs to the generalized plant P and are the values according to which the disturbance is rejected. Our objective is to distinguish between high and low frequencies of the disturbance signal, and to independently allot the duty of high frequency disturbance rejection to the generator torque control input τ_e , and the low frequency disturbance rejection to the blade pitch control input β . The controller weights are weights or penalties imposed on the control inputs to ensure that the disturbance rejection function is successfully distributed amongst the control inputs depending according to the corresponding frequencies.

Thus W_u will be a 2x2 square matrix, with the first and second diagonal terms corresponding to weights on control inputs β and τ_e respectively. The secondary diagonal terms remain 0 since the control of β and τ_e are independent of each other. Thus the general structure of W_u is:

$$W_u = \begin{bmatrix} W_{u\beta} & 0 \\ 0 & W_{u\tau_e} \end{bmatrix}$$

where $W_{u\beta}$ corresponds to the weight on control input β , and $W_{u\tau_e}$ corresponds to the weight on control input τ_e . Now to decide what type of frequency filter weights we allot to the respective inputs, we first take a look at the input wind profile in Figure 14.

We can see that the input can be separated into one big low frequency sinusoid of time period

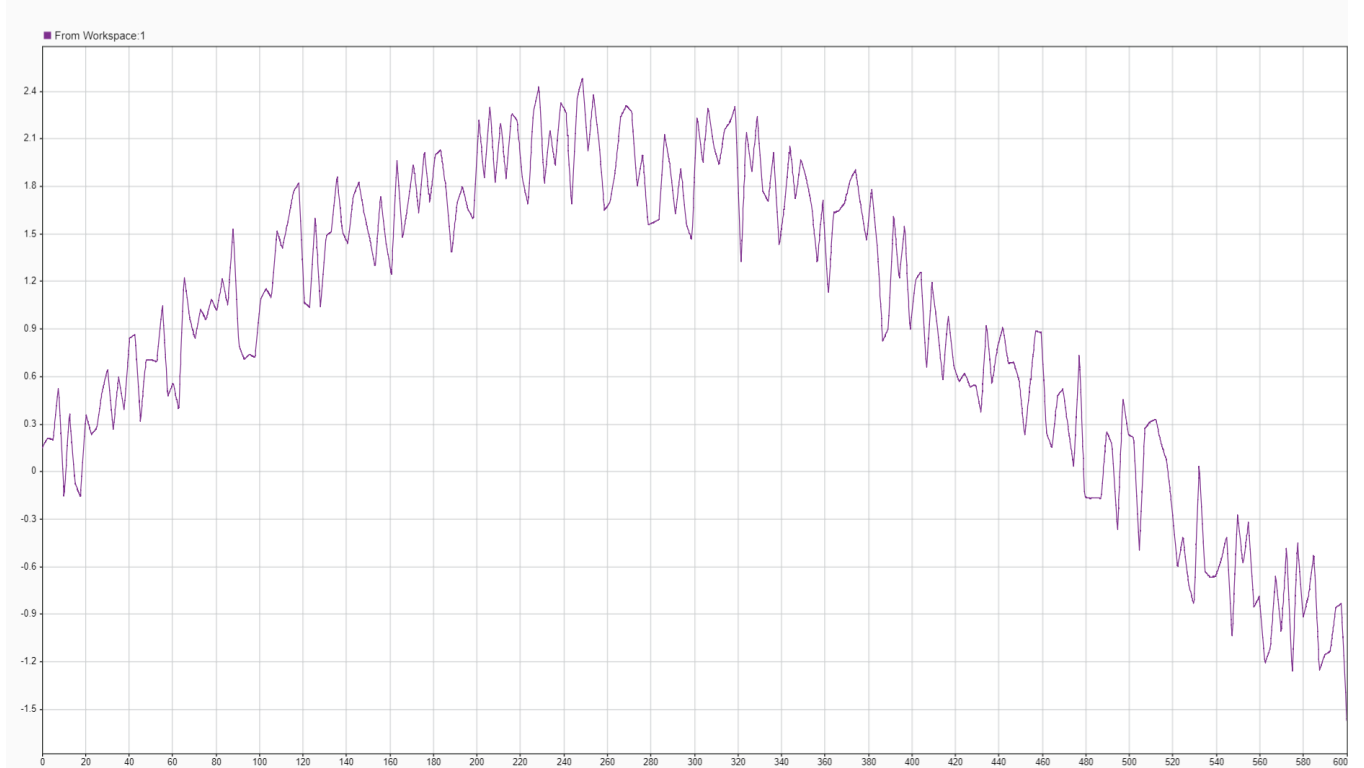


Figure 14: The Mixed-Frequency Wind Data Disturbance Input

approximately 1000 seconds, and multiple high frequency noises with time periods varying between 5 to 10 seconds. The 2 corresponding frequencies are around 0.001Hz and between 0.1Hz to 0.2Hz respectively. According to these frequencies we can decide the cut-off frequencies for our control weights. We want β to be the control input for the low frequency sine wave of period 1000s, and we want τ_e to be the control input for the high frequency signals. Therefore the control weight for β should be designed such that at low frequencies, the penalty or the gain imposed on β is low, and the penalty on β is high at high frequencies. Such a function corresponds to that of a high-pass filter, which has low gain at low frequencies and high gain at high frequencies. The converse of these requirements apply to the input τ_e . Since we want τ_e to operate at high frequencies, we need to impose

a high penalty at low frequencies, and a low penalty at high frequencies. These can be fulfilled by a low-pass filter, which has a high gain at low frequencies and a low gain at high frequencies.

Now that we have decided what type of filters we need to apply to which control inputs, we need to decide the cross-over frequencies of these filters. These are the frequencies at which the magnitude plot of the filter crosses the 0dB mark. Practically, this indirectly decides the frequency ranges above or below which we can consider our filter to be active. While in the previous question, to keep $\|N\|_\infty < 1$, we had to ensure that $\|W_p G_d S\|_\infty < 1$, now we need to ensure that $\|W_u K G_d S\|_\infty < 1$, where K is the controller. Thus we need to ensure that $|1/W_u|$ bounds $K G_d S$. Figure 15 shows the Bode magnitude plots of $K G_d S$. The upper plot corresponds to β , and the lower plot corresponds to τ_e .

Looking at the upper plot corresponding to β control input, we can see that we need a $|1/W_u|$

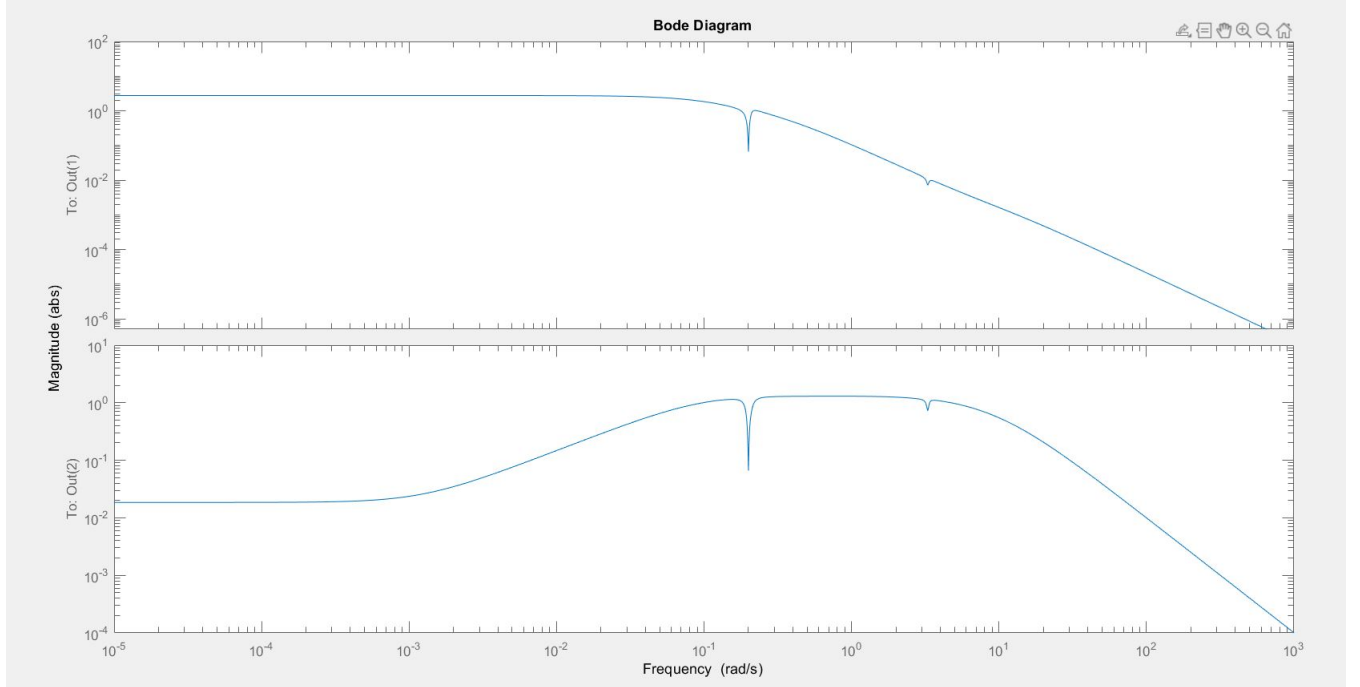


Figure 15: Bode plots of $K G_d S$

plot needed to bound the curve would be a high pass filter, and for the lower plot, a low pass filter can bound the curve. We decided to allot the same cut-off frequency to both the weights since it will be easier to classify control inputs corresponding to frequencies greater than or lesser than these frequencies. Since the time period of the low frequency is of the order 0.001Hz and the high frequencies are between 0.1 and 0.2Hz approximately, we decided to select 0.01Hz as the cut-off frequency of both the high-pass and low-pass filters. We desire that any frequency above 0.01Hz be classified as high frequency and let generator torque perform control action. For the frequencies less than 0.01Hz, the control action should be performed by β . Thus, the controller weight matrix W_u that we choose which satisfies all these requirements are

$$W_u = \begin{bmatrix} \frac{100(s+0.0006283)}{(s+6.283)} & 0 \\ 0 & \frac{0.01(s+6.284)}{(s+0.001257)} \end{bmatrix}$$

which are generated using the **makeweight** function. Thus, using the weights mentioned above, we achieve $\|W_p K G_d S\|_\infty < 1$ as desired, with some limitations.

2.4 Question 4

Using the **hinfsyn()** we synthesize our H_∞ controller using the generalized plant P as the input to the function. The output of this function is the H_∞ controller K , which takes in the error input ($-w_r$, and gives 2 outputs(corresponding to β and τ_e). These 2 outputs are inputs to the plant G , whose output is w_r . This output is added to the disturbance G_{dd} and that is our output signal.

We have previously defined the values of W_u and W_p that we selected for our task. In the previous sections we have seen the bode plots of our controllers and errors and have elucidated the weighting selection procedure for the same. Now we evaluate the weights we have selected.

The first plot is the bode magnitude plot of the controller corresponding to the control input β versus the magnitude plot of its corresponding weight in W_u .This is shown in Figure 16. We can

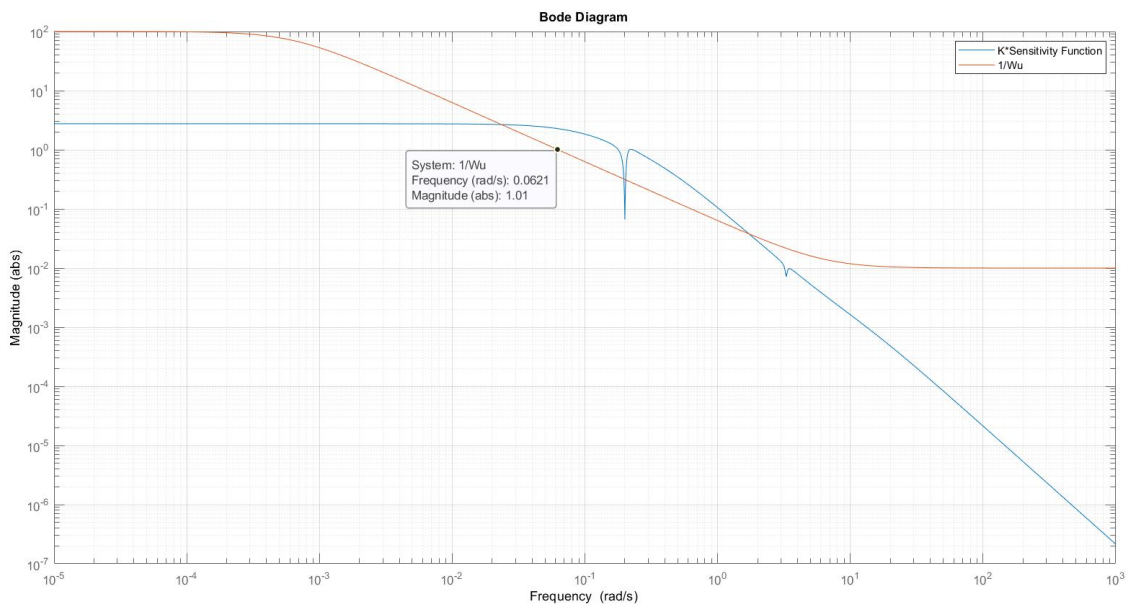


Figure 16: Bode magnitude plots of β controller vs corresponding controller weight $1/W_u$

see that for most of the frequency ranges, the weight provides a very good bound on the controller transfer function. The shape of the control weight is as desired($1/W_u$ is a LP filter, which means W_u is a HP filter), and this provides a pretty good robust performance where $\|K W_u G_d S\|_\infty < 1$.

The next plot we analyse is the bode magnitude plot of the controller corresponding to the control input τ_e versus the magnitude plot of its corresponding weight in W_u .This is shown in Figure 17. We can see that this weight provides a very good bound on the controller transfer function. The shape of the control weight is as desired($1/W_u$ is a HP filter, which means W_u is a LP filter), and this provides a pretty good robust performance where $\|K W_u G_d S\|_\infty < 1$. Thus, both the controller weights provide sufficient bounds on their corresponding controller actions in order to ensure a good performance.

The error weights provide several problems while designing, which were previously highlighted. Due to sensitivity issues, the desired closed loop bandwidth had to be chosen carefully. The bode magnitude plot of the error($-w_r$) versus the magnitude plot of its error weight in W_p is shown in Figure 18. This error weight, due to limitations on sensitivity, and correspondingly the bandwidth, does not provide such a good bound on the sensitivity curve. However, the shape is as desired, and considering that the output w_r is of the order of 180rad/s, a little extra tolerance for error is permissible, as long as there is no compromise on the sensitivity.

In the next section, we simulate our system for disturbance rejection with these weights and observe

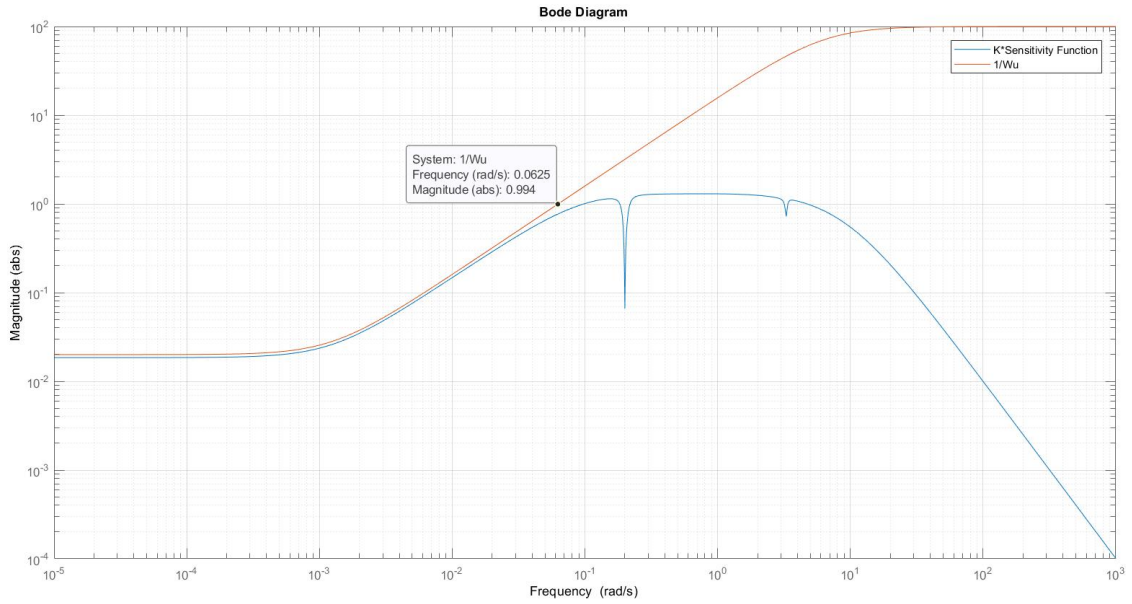


Figure 17: Bode magnitude plots of τ_e controller vs corresponding controller weight $1/W_u$

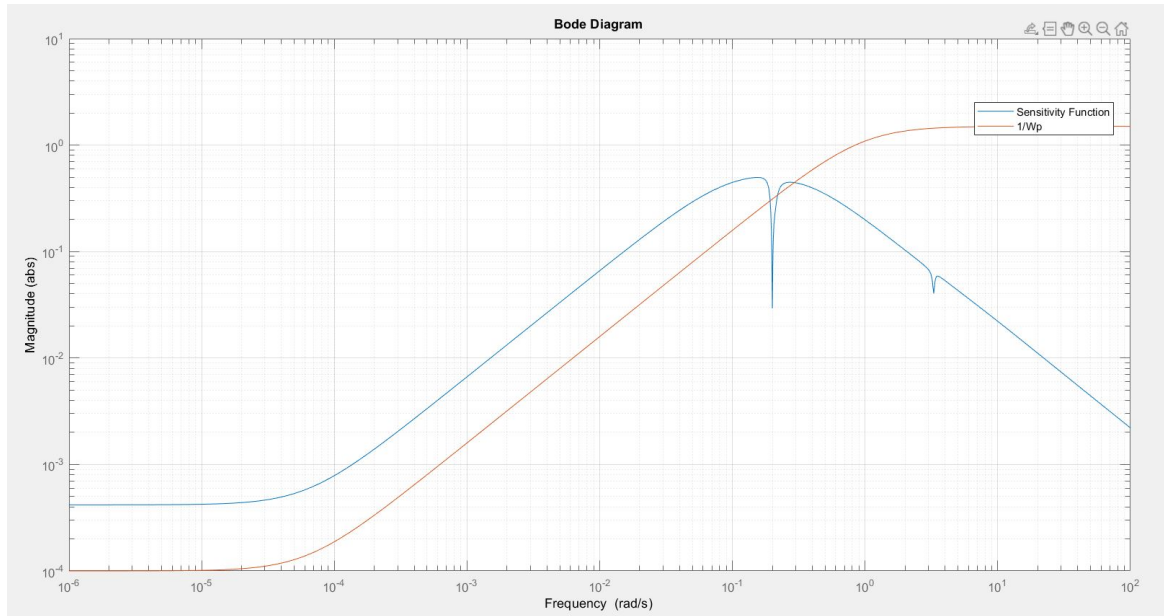


Figure 18: Bode magnitude plots of w_r error vs error weight $1/W_p$

that these weights are sufficient to provide a very good performance.

2.5 Question 5

After synthesizing the controller, we have performed all the time domain simulations using Simulink. Our Simulink block diagram is as shown in Figure 19.

Wind_Data block is the non-linear disturbance input provided. Under that is a sine wave generator

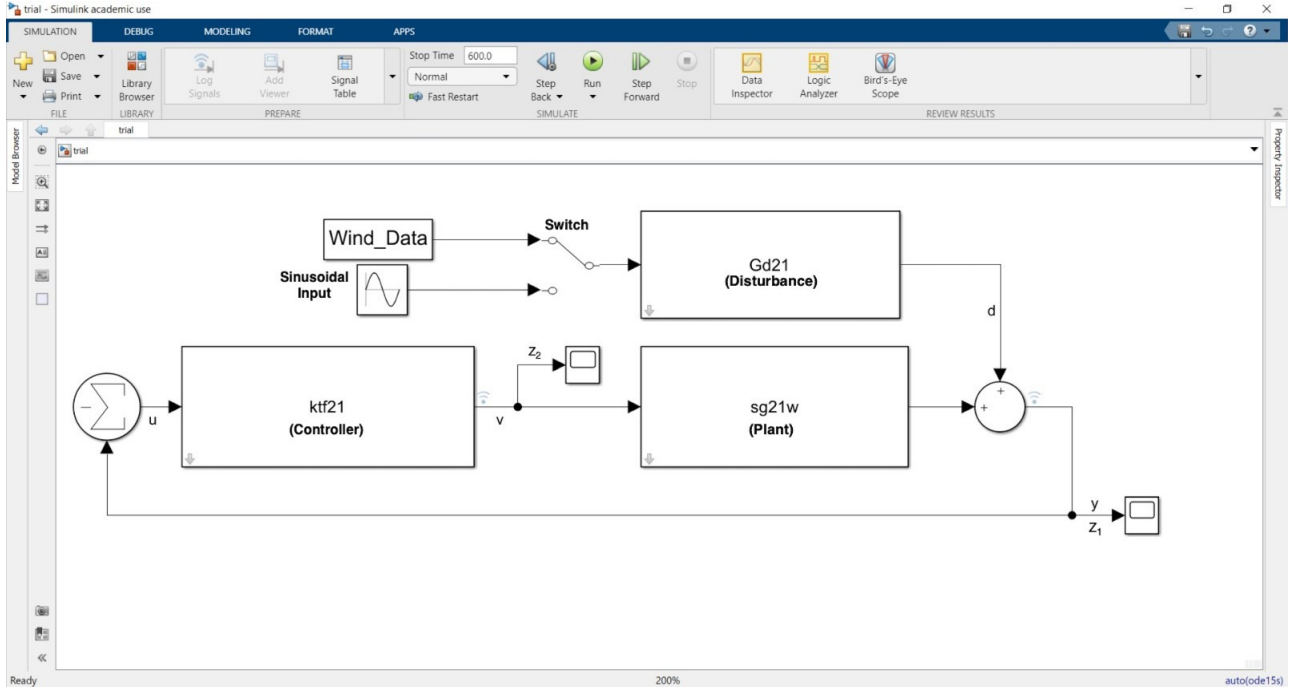


Figure 19: Simulink diagram of the system

whose frequency and amplitude can be varied as desired. The manual switch is used to manually switch between using the sine wave as an input source or our original wind data. These inputs pass through the Disturbance transfer function before being added to the output as disturbance. The controller and plant are placed such that the output of the controller is connected in negative feedback to the input of the controller. According to the generalized plant structure, our output z_2 is at the output of the controller, and z_1 is at the output of the plant after disturbance has been added. Scopes have been placed at both these outputs, however it is preferred to use the data inspector icons placed near each block, as they provide better, more lucid outputs.

We first run the simulation with the original Wind_Data. The output at z_1 is as shown in Figure 20. Since this is a plot of disturbance rejection of w_r versus time, the desired output is one that settles at 0, with minimal errors. The errors of our output do not exceed 0.3 rad/s, which is negligible when compared to the rated rotational velocity of 180 rad/s. This output shows that the controller and error weights designed work as desired.

The control actions for this simulation are as shown in Figure 21.

$v(1)$, which is the plot in blue, corresponds to the control action of the β control input. $v(2)$, which is the plot in red, corresponds to the control action of the τ_e control input. As we can see from Figure 21, the control actions replicate almost exactly what we desire. The β control input should be operating only at low frequencies, and as $v(1)$ confirms, the control action of β is a high magnitude, slightly noisy sine wave of time period around 1010 seconds. On the other hand, the τ_e control input should be operating only at high frequencies, and as $v(2)$ confirms, the control actions of τ_e are of high frequency, small magnitude, noisy signals, which is exactly as desired. From these time domain outputs and simulations we can conclude that our H_∞ controller, the controller weights and error weights work exactly as desired, while also maintaining the robustness of the system.

To confirm that our controllers are working exactly as desired, we will separately apply a high frequency and a low frequency noiseless sine wave as the disturbance input to our system and monitor the corresponding control actions.

What we desire is that when we apply only a low frequency noiseless sine wave as the disturbance

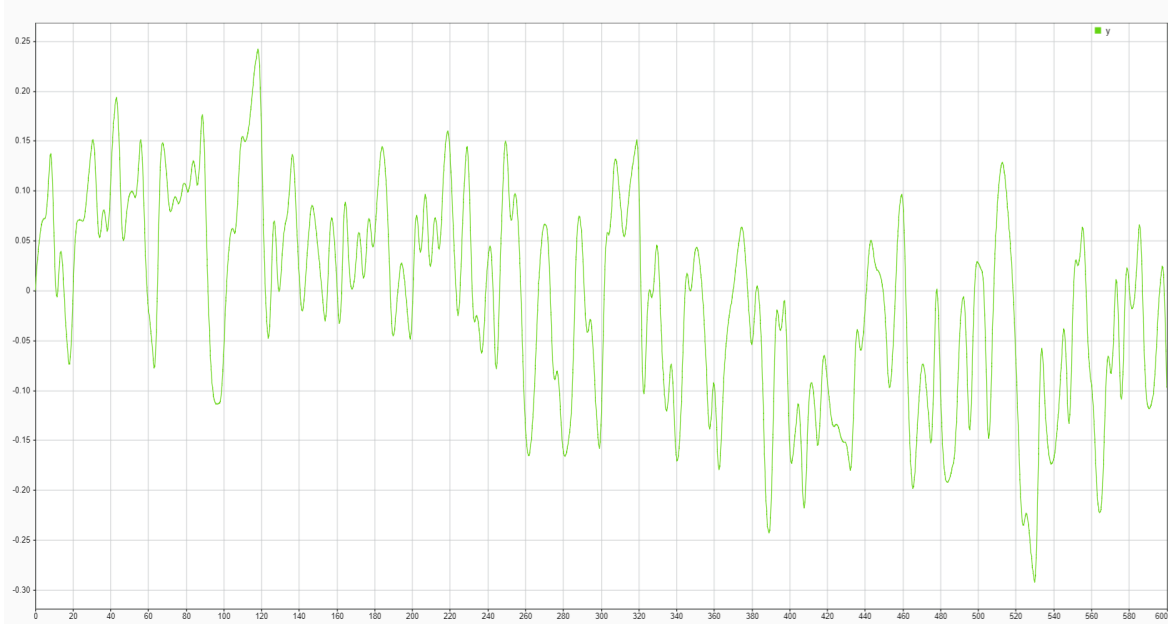


Figure 20: Output when using Wind_Data as input

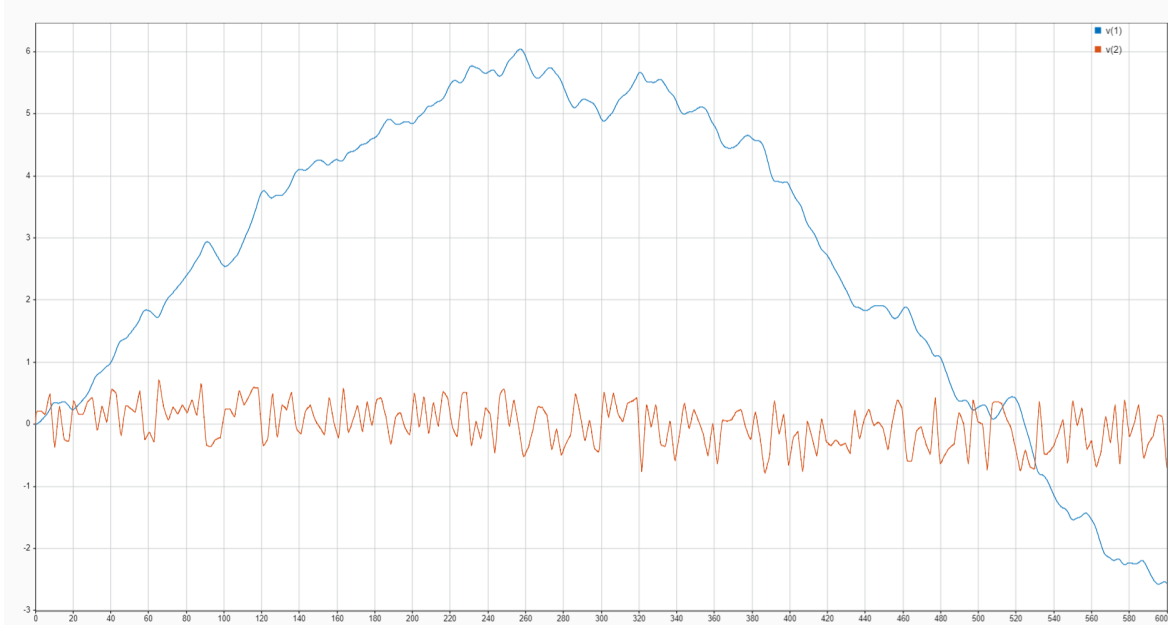


Figure 21: Control Actions when using Wind_Data as input

input, it should be rejected, with most of the control action being performed by the low frequency controller(β control input), while when we apply only a high frequency noiseless sine wave as the disturbance input, it should be rejected, with most of the control action being performed by the high frequency controller(τ_e control input).

We first apply a noiseless sine low frequency sine wave with amplitude 1, and frequency 0.005rad/s. The input signal is as shown in Figure 22.

The disturbance rejection plot is shown in Figure 23 with the sine wave input in the background. The green line indicates the output. It can be seen that the disturbance is rejected very well, with very little errors.

Lastly, we plot the control actions of the controllers. Looking at the input, we expect a big contribution from the β control input, and a small one from τ_e . Figure 24 shows the control actions.

$v(1)$ is the blue line corresponding to the control input β 's action, while the pink curve $v(2)$ corresponds to τ_e 's control action. The results tally with our expectations as we observe that β is the

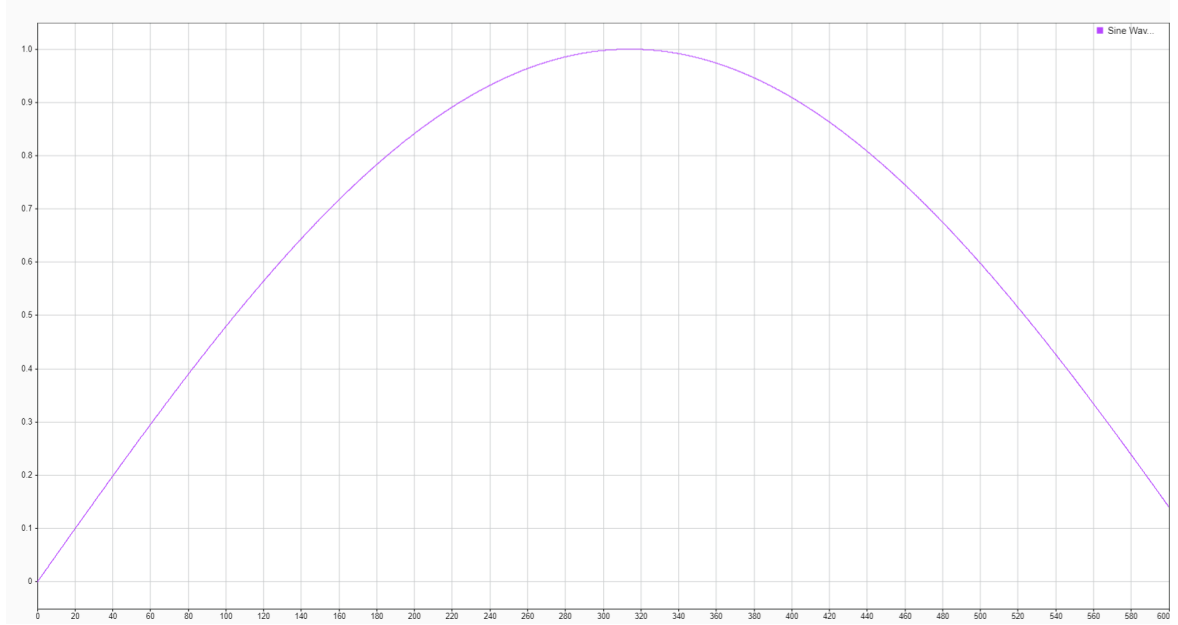


Figure 22: Low Frequency Noiseless Sine Input

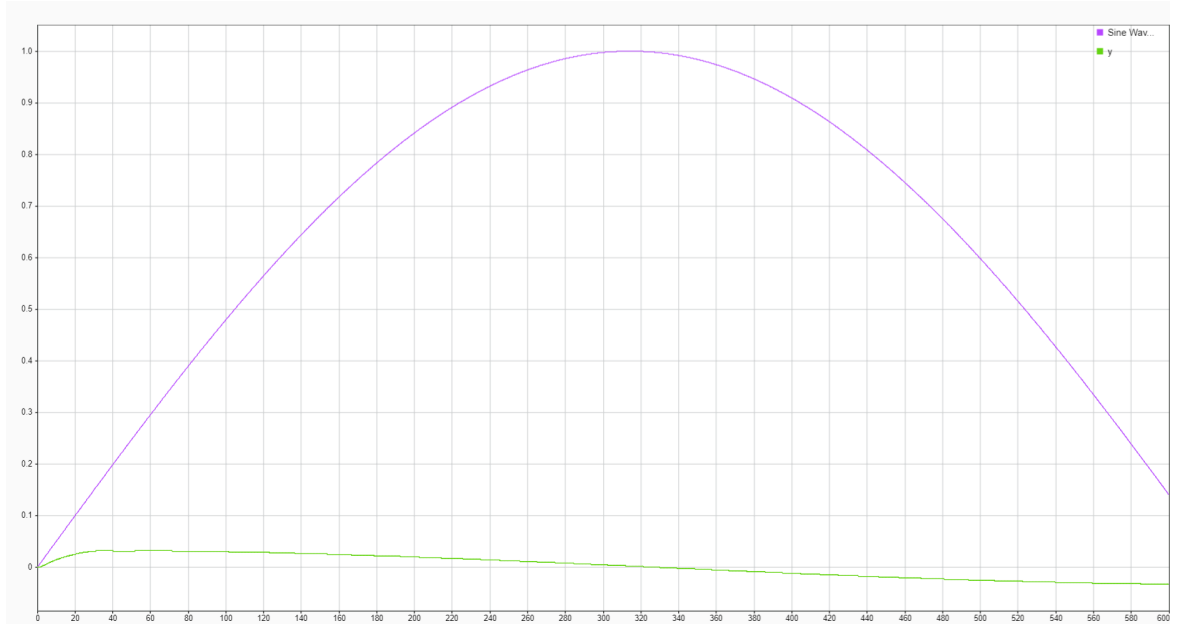


Figure 23: Output with Low Frequency Noiseless Sine Input

main controller here, and τ_e contributes next to nothing to reject this low frequency disturbance.

Now we apply a noiseless sine high frequency sine wave with amplitude 1 at the disturbance channel, with frequency 1rad/s. The input signal is as shown in Figure 25.

The disturbance rejection plot is shown in Figure 26 with the sine wave input in the background. The green line indicates the output. It can be seen that the disturbance is rejected well, with little errors, and a persistent oscillation about the steady state.

Lastly, we plot the control actions of the controllers. Looking at the input, we expect a big contribution from the τ_e control input, and a small one from β . Figure 27 shows the control actions.

$v(1)$ is the blue line corresponding to the control input β 's action, while the red curve $v(2)$ corresponds to τ_{e_1} 's control action. The results tally with our expectations as we observe that τ_e is the main controller here, and β contributes next to nothing to reject this high frequency disturbance. Thus, we can conclude that our control system successfully differentiates between a high frequency

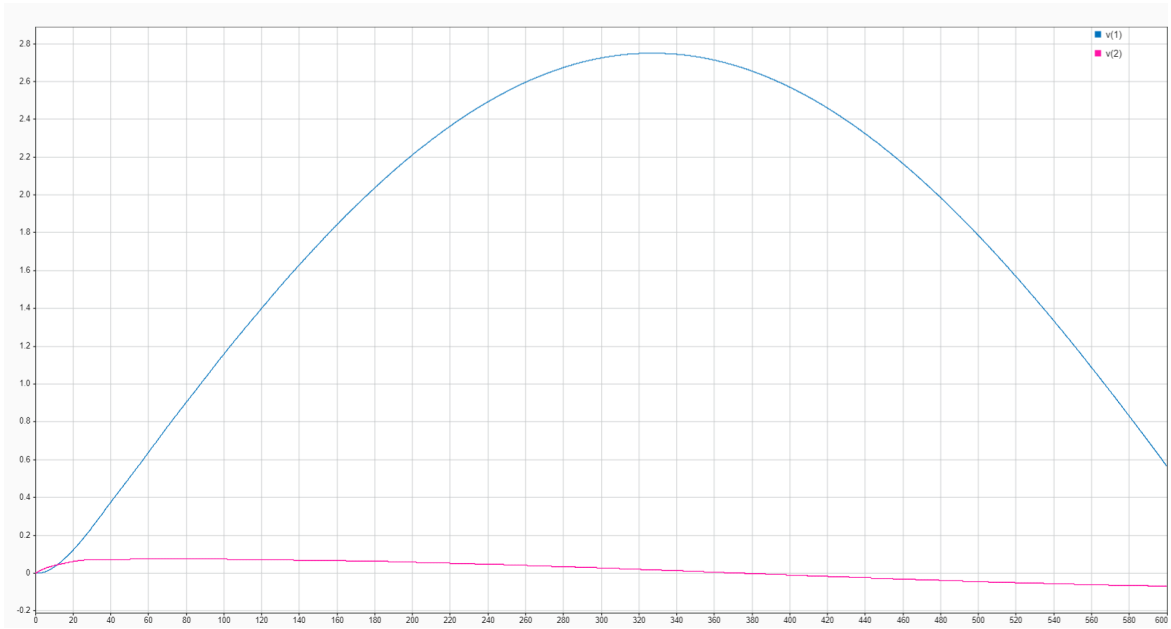


Figure 24: Control Actions with Low Frequency Noiseless Sine Input



Figure 25: High Frequency Noiseless Sine Input

and a low frequency disturbance, successfully distributes the work between the blade pitch control and generator torque control depending on the frequency, and successfully rejects the disturbance. Thus, we successfully counteract the change in rotational velocity w_r , by changing either the blade pitch or generator torque, thus keeping the turbine running at its rated power $w_r \cdot \tau_e$. We successfully designed efficient controller weights and error weights, while respecting the physical limitations of the system, and maintaining its robustness, while also ensuring a near-optimal performance.



Figure 26: Output with High Frequency Noiseless Sine Input



Figure 27: Control Actions with High Frequency Noiseless Sine Input